2018

Influence of the estrous cycle and female sex hormones on GHB toxicokinetics

Hao Wei
University of the Pacific

INFLUENCE OF THE ESTROUS CYCLE AND FEMALE SEX HORMONES ON GHB TOXICOKINETICS

by

Hao Wei

A Thesis Submitted to the

Graduate School

In Partial Fulfillment of the

Requirements for the Degree of

MASTER OF SCIENCE

Thomas J. Long School of Pharmacy and Healthy Sciences
Pharmaceutical and Chemical Sciences

University of the Pacific
Stockton, California

2018

INFLUENCE OF THE ESTROUS CYCLE AND FEMALE SEX HORMONES ON GHB TOXICOKINETICS

By

Hao Wei

APPROVED BY:

Thesis Advisor: Melanie A. Felmlee, Ph.D

Committee Member: Miki S. Park, Ph.D

Committee Member: Roshanak Rahimian, PharmD, Ph.D

Department Chair: William K. Chan, PharmD, Ph.D

Dean of Graduate School: Thomas Naehr, Ph.D

ACKNOWLEDGEMENTS

Thank to Dr. Miki S. Park and Dr. Roshanak Rahimian for suggestion of thesis writing.

Thank to Fang Liu for her assistance in modification of LC-MS/MS method.

Influence of the Estrus Cycle and Female Sex Hormones on GHB Toxicokinetics

Abstract

By Hao Wei

University of the Pacific
2018

Gamma-Hydroxybutyrate (GHB) is an endogenous short-chain fatty acid formed from Gamma-aminobutyric acid (GABA). Clinically, GHB is marketed in the United States as Xyrem to treat narcolepsy with cataplexy and in Europe for the treatment of alcohol withdrawal and narcolepsy. However, the illicit use and abuse of GHB occurs due to its sedative/hypnotic and euphoric effects. Monocarboxylate transporters (MCTs and SMCTs) are integral membrane proteins that control the bidirectional transport of endogenous substrates including lactate, acetate and pyruvate. They have also been found to transport and mediate the clearance and distribution of GHB. MCTs demonstrate a wide tissue distribution, including brain, kidney, liver, and intestine, all of which play an important role in determining the disposition of GHB.

Sex differences in drug elimination pathways contribute to the wide range of inter-individual variability observed between sexes with respect to drug disposition and effect. Sex differences in MCT expression have been observed in the brain, muscle, liver and kidney with variations potentially driven by sex hormones; however, there is an absence of information on how these expression differences translate into sex differences in GHB toxicokinetics. The objective of this study was to evaluate sex differences and the influence of the estrus cycle on GHB toxicokinetics after IV administration. Our hypothesis is that renal clearance and

toxicokinetics will vary over the estrus cycle. Estrus cycle stage in female rats was determined by vaginal lavage prior to GHB administration. Ovariectomized (OVX) females were included in the study to evaluate GHB toxicokinetics in the absence of female sex hormones. Our results demonstrated that sex and the estrus cycle influence GHB toxicokinetics. Total and renal clearance varies over the estrus cycle with the highest renal clearance observed in proestrus females. In contrast, males and OVX females demonstrated significantly lower renal clearance. These results suggest that GHB toxicity and risk of overdose varies over the estrus cycle due to expression changes in renal MCTs and SMCTs. Future studies will evaluate higher GHB doses to determine the role of sex hormones in GHB overdose and fatality. In addition, hormone replacement studies will be conducted to confirm the role of individual sex hormones on GHB toxicokinetics.

TABLE OF CONTENTS

LIST OF TABLES

Table

LIST OF FIGURES

Figure

Chapter 1: Introduction

1.1 GHB

γ-hydroxybutyrate (GHB), also known as γ-hydroxybutyric acid, 4-hydroxybutyric acid, 4-hydroxybutanoic acid, is an endogenous four carbon chain fatty acid (X. Wang, Q. Wang, & M. E. Morris, 2008). GHB is produced from γ-aminobutyric acid (GABA), which acts as a neurotransmitter (Felmlee, Wang, et al., 2010). GHB is a neuromodulator in the central nervous system , and interacts with the GHB and $GABA_B$ receptors (Schep, Knudsen, Slaughter, Vale, & Megarbane, 2012). GHB is used clinically as Xyrem (sodium oxybate; Jazz Pharmaceuticals) to treat narcolepsy with cataplexy in America (Felmlee, Roiko, Morse, & Morris, 2010), and to treat alcohol withdrawal, heroin dependence, sleep disorders and narcolepsy in Europe (Boscolo-Berto et al., 2012; Felmlee, Wang, et al., 2010). GHB, is most famous for its illicit use and abuse in night clubs and raves and drug-facilitated sexual assault because of its sedative/hypnotic and euphoric effects (X. Wang et al., 2008). GHB is colorless, odorless and tasteless, and has high solubility, therefore it is easy to unknowingly administer a high dose. The dose-response curve for GHB is very steep; minor increases in dose can lead to significant adverse events. Toxicological effects of GHB include dizziness, respiratory depression, vomiting, and unconsciousness, as well as coma and death (Felmlee, Roiko, et al., 2010).

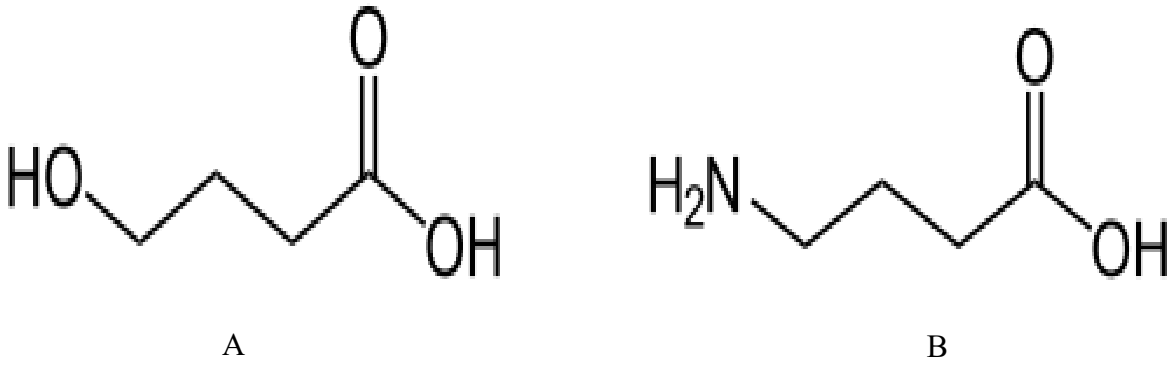

A B

Figure 1: Chemical structure of (A) GHB and (B) GABA.

In Europe, the Drug Emergencies Network found that the top 5 drugs involved with emergency department visits from September 2013 to September 2014 were heroin (1345 visits), cocaine (954 visits), cannabis (904 visits), GHB (711 visits), and amphetamines (593 visits) (White, 2017). Similarly, in Norway, there were 2923 episodes of acute poisoning from 2011 to 2012 in an emergency clinic and GHB accounted for 5% of the total (White, 2017). In the USA, more than 7100 GHB overdose cases and 65 GHB related deaths were reported from 1990 to 2000 (Shannon & Quang, 2000). Although GHB has been strictly controlled as a schedule I drug since 2000 in America (Felmlee, Wang, et al., 2010), it is still readily obtained and is also formed in vivo from either 1,4-butanediol (BD) or γ-butyrolactone (GBL), which can be obtained legally as industrial material (Fung et al., 2008).

The range of GHB doses typically seen in humans in abuse and overdose cases ranges between 18 and 250 grams (Y. G. Wang, Swick, Carter, Thorpy, & Benowitz, 2009). Therapeutic doses of sodium oxybate for narcolepsy range from 4.5 to 9 grams per night

(Kantrowitz, Citrome, & Javitt, 2009). Case reports and case series regarding the features of GHB poisoning provide a relatively consistent result for GHB toxicity in humans. When the GHB dose is below 10 mg/kg, there will be mild clinical effects, such as short-term anterograde amnesia, hypotonia, and euphoria (Schep et al., 2012). Drowsiness, sleep, and myoclonus can occur following a dose of 20 - 30 mg/kg (Schep et al., 2012), whereas doses of 50 mg/kg and higher can lead to coma (Schep et al., 2012). Doses over 50 mg/kg can result in the onset of coma, bradycardia, and/or respiratory depression (Schep et al., 2012). Thus, patients may present with symptoms ranging from sudden drowsiness to unresponsive and profound coma, determined by the dose ingested. In rats, a dose of 200 mg/kg induces sleep and respiratory depression with lethality observed at 1750 mg/kg (Felmlee, Roiko, et al., 2010; Morse, Vijay, & Morris, 2012). Currently, there are no clinically available therapies to treat GHB overdose, and care focuses on symptom treatment until the drug is cleared from the body.

1.2 GHB Toxicokinetics

GHB toxicokinetics are nonlinear both in rats and humans with capacity-limited metabolism, renal clearance and oral absorption (Abanades et al., 2006; Felmlee, Wang, et al., 2010; Ferrara et al., 1992; Lettieri & Fung, 1979; Palatini et al., 1993; X. Wang et al., 2008). In humans, at a dose range of 40 – 72 mg/kg, GHB elimination is non-linear with clearance parameters dependent on the dose administered (Abanades et al., 2006; Palatini et al., 1993). As Figure 2A illustrates, GHB has a non-linear concentration versus time profile in rats following intravenous administration of 200 to 1000 mg/kg resulting from saturable metabolism and renal clearance (Felmlee, Wang, et al., 2010; Lettieri & Fung, 1979). In rats, GHB metabolic clearance was saturated at all doses evaluated with a predicted in vivo K_m for metabolism of 0.054 mg/ml (Felmlee, Wang, et al., 2010). As GHB dose is increased, the renal clearance of GHB increases

(Figure 2B). These dose-dependent increases in renal clearance suggest active, transporter-mediated, renal reabsorption of GHB (Felmlee, Wang, et al., 2010; Morris, Hu, & Wang, 2005).

GHB given by the oral route is rapidly absorbed. In rats, the plasma concentrations of GHB plateau for a long time after oral administration due to saturation of intestinal absorption and continuous absorption along the length of the intestine and colon (Morse & Morris, 2013a, 2013b; Vijay, Morse, & Morris, 2015). Due to saturation of intestinal transport, bioavailability of GHB is nonlinear with decreased bioavailability with increasing dose (Lettieri & Fung, 1979). GHB metabolism and renal clearance are also saturated at the doses given in oral administration studies (Morse & Morris, 2013a, 2013b; Vijay et al., 2015). GHB is widely distributed in the body with measureable concentrations in the mammalian brain, liver, kidney, intestine and other peripheral tissues, and demonstrates tissue-specific nonlinear distribution consistent with the involvement of monocarboxylate transporters (Felmlee, Morse, Follman, & Morris, 2017).

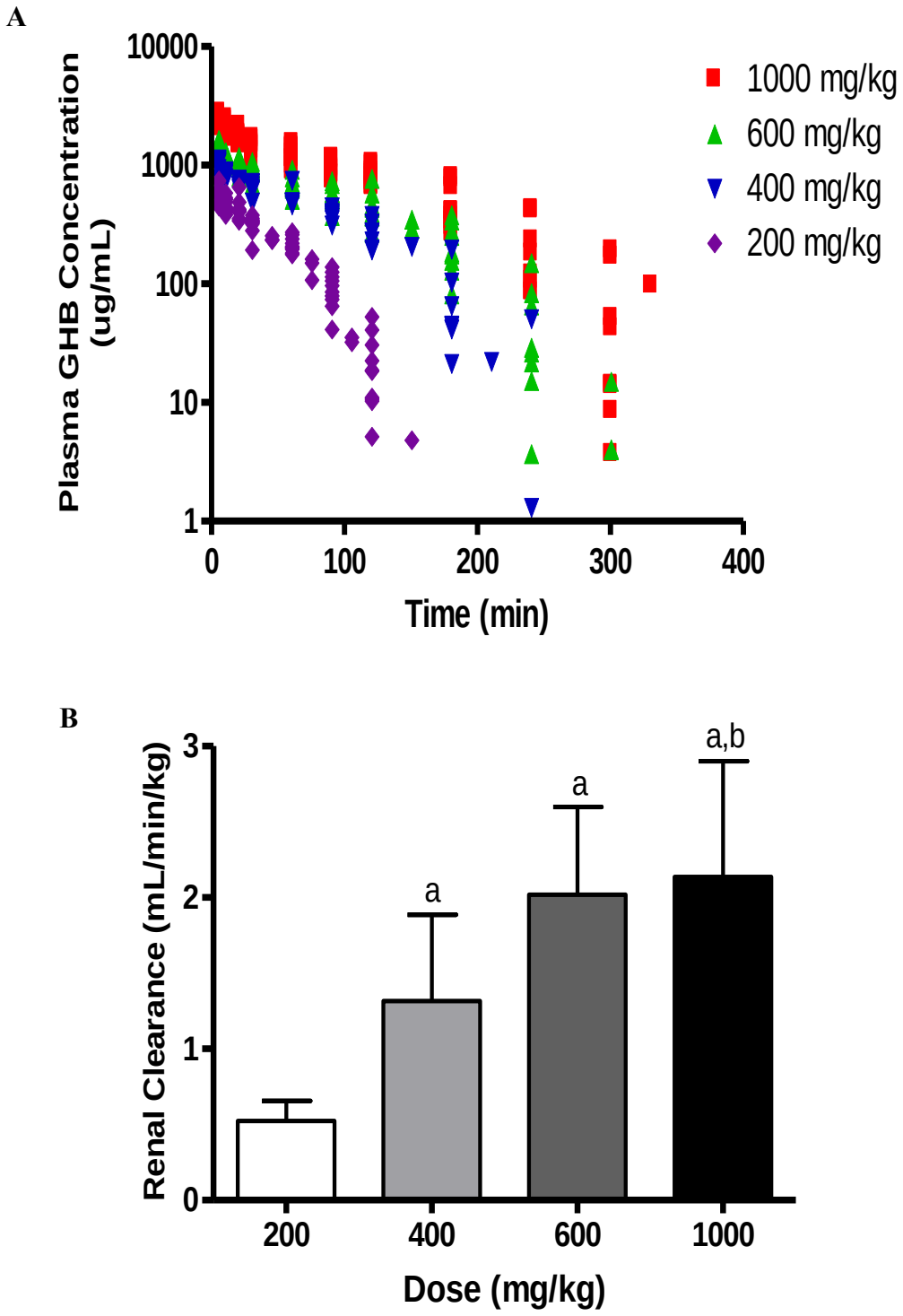

Figure 2: Dose-dependent GHB plasma concentration versus time profiles and renal clearance after IV administration in rats [data from (Felmlee, Wang, Cui, Roiko, & Morris, 2010)]. P^a <0.05 compared to 200mg/kg; P^b <0.05 compared to 400mg/kg.

1.3 Monocarboxylate Transporters

Monocarboxylate transporters belong to the SLC16A family of proton-coupled monocarboxylate transporters (MCTs) and the SLC5A family of sodium-coupled monocarboxylate transporters (SMCTs). The SLC16A family was first identified in the mid-nineties, as transporters of endogenous monocarboxylic acids (Morris & Felmlee, 2008). Based on sequence homology, fourteen MCT-related genes of this family have been identified in mammals (Morris & Felmlee, 2008). Of the 14 identified members, eight MCTs have been functionally characterized: MCTs 1-4, MCT6, MCT8, MCT10, and MCT12 (Morris & Felmlee, 2008; Schwartz & Stevenson, 2007). MCTs have a wide tissue distribution including the liver, stomach, colon, ileum, and kidney, likely due to their role in the transport of endogenous monocarboxylates which function as cellular energy sources (Morris & Felmlee, 2008). MCTs may be located on basolateral or apical membrane depending on the specific cell type (Morris & Felmlee, 2008).

MCTs 1 - 4 are the most abundant and widely studied, and are the only members of the family that demonstrate proton-coupled transport of monocarboxylates. MCT1 - 4 transport endogenous and exogenous compounds including lactate, pyruvate, butyrate, acetate, valproic acid, GHB, and pravastatin (Morris & Felmlee, 2008). Other characterized MCTs have been demonstrated to transport a wide variety of endogenous and/or exogenous compounds: MCT6 is a transporter of bumetanide, nateglinide, and probenecid; MCT8 is transporter of thyroid hormones; MCT10 is transporter of aromatic amino acids; and MCT12 is transporter of creatinine (Jones & Morris, 2016).

MCT1 (SLC16A1) was the first member of MCT family to be identified (Jackson, Price, & Halestrap, 1995). The proposed topological structure of MCT1 has 12 transmembrane helices

with intracellular C- and N-termini (Halestrap, 2013; Halestrap & Price, 1999). MCT1 in a closed conformation has cytosolic substrate binding site, and in the open conformation has an extracellular substrate binding site (Halestrap, 2013). DIDS, and MCT inhibitor, is proposed to interact with four extracellular lysines residues of MCT1 (K38, K45, K282 and K413) (Halestrap, 2013). This topology is predicted to be shared by all members of the SLC16 family; however, to-date no crystal structures are available for any SLC16Amembers or SLC5A8 or SLC5A12.

Within the SLC5A family, two sodium-couple monocarboxylate transporters have been identified: SLC5A8 (SMCT1) and SLC5A12 (SMCT2). SMCT1 was first identified in 2003 by Li et al. (Li et al., 2003) , and SMCT2 was identified in 2005 by Srinivas et al. (Srinivas et al., 2005). SMCT1 and 2 are predominantly expressed in intestine and kidney, with no expression demonstrated in other tissues (20). SMCTs are typically expressed on the apical membrane of the cell (Iwanaga & Kishimoto, 2015). In contrast to MCTs, which function as H^+-coupled electroneutral transporters, SMCTs function as Na^+-coupled electrogenic transporters with SMCT1 having a 2:1 transport ratio (Na^+:substrate) (Cui & Morris, 2009). Although there is no structural similarity between MCT1 and SMCT (Ganapathy et al., 2008), and the transport mechanism is different as well between the two transporters, both of transporters have similar substrate specificity (Ganapathy et al., 2008). Endogenous substrates of SMCTs include lactate, acetate, propionate, and butyrate (Ganapathy et al., 2008; Iwanaga & Kishimoto, 2015). SMCTs also functions as drug transporters to regulate the intestinal absorption and renal clearance of various monocarboxylate drugs including GHB, salicylates, benzoate, and non-steroidal anti-inflammatory drugs (Ganapathy et al., 2008; Iwanaga & Kishimoto, 2015).

1.4 Monocarboxylate Transporters and GHB Toxicokinetics

GHB is a substrate for MCTs and SMCTs. It has been demonstrated that MCT inhibition is a potential treatment strategy for GHB overdose by inhibiting its active renal reabsorption mediated by MCTs and SMCTs and subsequently increasing GHB renal clearance (Morris et al., 2005; Morris et al., 2011; Vijay et al., 2015). Administration of MCT inhibitors such as L-lactate results in an increase in GHB renal and total clearance in rats (Roiko, Vijay, Felmlee, & Morris, 2013a; Q. Wang, X. Wang, & M. E. Morris, 2008). Similarly, after luteolin treatment, the renal and total clearances of GHB are significantly increased because of inhibition of the MCT1-mediated renal reabsorption (Q. Wang & Morris, 2007). As well, some immunosuppressive compounds such as AR-C117977 and AR-C122982 (Pahlman et al., 2013) have been identified as potent MCT inhibitors to increased GHB renal and total clearance (Vijay et al., 2015).

The sedative/hypnotic effects of GHB and respiratory depression were seen during overdose resulting from its effects in the brain (Morse et al., 2012; Roiko et al., 2013a). In brain, GHB can interact with GHB – specific receptor and $GABA_B$ receptor (Morse et al., 2012; Roiko et al., 2013a) .It has been demonstrated GHB exhibits uptake into the frontal cortex which is mediated by MCT and was saturated at high GHB concentrations (Roiko, Felmlee, & Morris, 2012). Administration of MCT inhibitor L-lactate decreased brain extracellular fluid concentration of GHB and decreased sedative/hypnotic effects (Roiko et al., 2013a).

Variations in MCT/SMCT expression in the kidney can alter renal reabsorption and renal clearance of GHB (Felmlee, Dave, & Morris, 2013; Felmlee, Wang, et al., 2010). Higher MCT/SMCT expression will lead to a greater amount of GHB being reabsorbed into systemic circulation, therefore the total amount of GHB excreted in the urine and GHB renal clearance are

lower (Felmlee et al., 2013). In contrast, lower MCT/SMCT expression will lead to the higher renal clearance and an increase in total GHB elimination.

1.5 Sex Differences in MCT Expression

The estrus cycle is the reproductive cycle in mammalian females and consists of varied exposure to female sex hormones. Previous studies show that the estrus cycle in female rats can be divided into four stages (Figure 3): proestrus, estrus, metestrus, diestrus (Cora et al., 2015). In different stages, plasma sex hormone concentrations are different and may contribute to differences in transporter expression (Haim, Shakhar, Rossene, Taylor, & Ben-Eliyahu, 2003). The highest concentrations of estrogen and progesterone are observed in the proestrus stage (Figure 3 from (Lebron-Milad & Milad, 2012)).

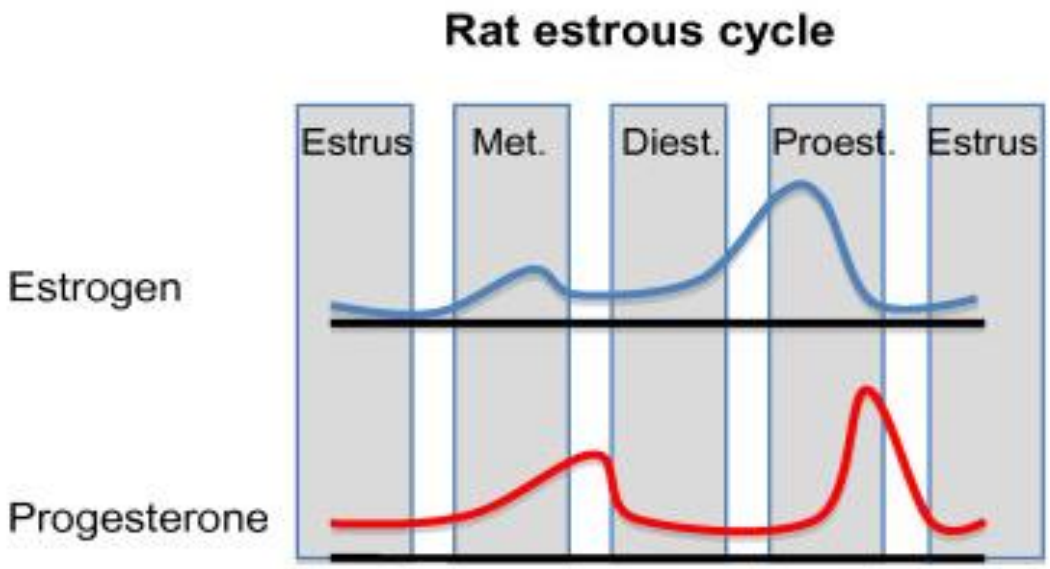

Figure 3: Hormone exposure over the estrus cycle [from (Lebron-Milad & Milad, 2012)].

There is limited literature data evaluating sex differences and the influence of sex hormones on MCT expression. Sex differences in MCT expression have been observed in the muscle, brain, and Sertoli cells with variation driven by sex hormones (Enoki, Yoshida, Lally, Hatta, & Bonen, 2006; Manente et al., 2015; Rato et al., 2012). Administration of testosterone increased MCT1 and MCT4 protein expression in rat skeletal muscle; however, expression was not altered in the heart suggesting tissue specific hormonal regulation mechanisms (Enoki et al., 2006). Further, it has been demonstrated that oestrogen-related receptor alpha (ERRα) expression can modulate the expression of MCT1 in mice (Aveseh, Nikooie, & Aminaie, 2015), while the induction of estrogen receptor β (ERβ) expression result in the expression of MCT4 in cell level in mesothelioma cells of mice (Manente et al., 2015). Ovariectomy (OVX) induced a decrease of

MCT2 expression in brain of mice (Manente et al., 2015) suggesting that female sex hormones are involved in MCT regulation.

There is a lack of data evaluating the influence of sex and sex hormones on MCT/SMCT expression in drug distribution tissues. Our laboratory has previously demonstrated that MCT1 and MCT4 hepatic expression varies between males and females, over the estrus cycle and in the absence of female sex hormones (Figure 4 from (Cao et al., 2017)). In the liver of rats, MCT1 membrane expression shows a significant difference in cycling females as compared to males and OVX females. The proestrus MCT1 membrane expression is the lowest and was significantly lower than OVX females (Cao et al., 2017). Females in the other estrus stages had higher MCT1 expression than proestrus females, but still lower compared to males and OVX females (Cao et al., 2017). Membrane expression of MCT4 was also significantly different between sexes with all females having lower expression than males with proestrus females having significantly lower expression than males (Cao et al., 2017). Our results suggest that expression of individual MCTs are differentially regulated by sex hormones. Preliminary work in our laboratory has also demonstrated that both male and female sex hormones influence intestinal and renal expression of MCTs.

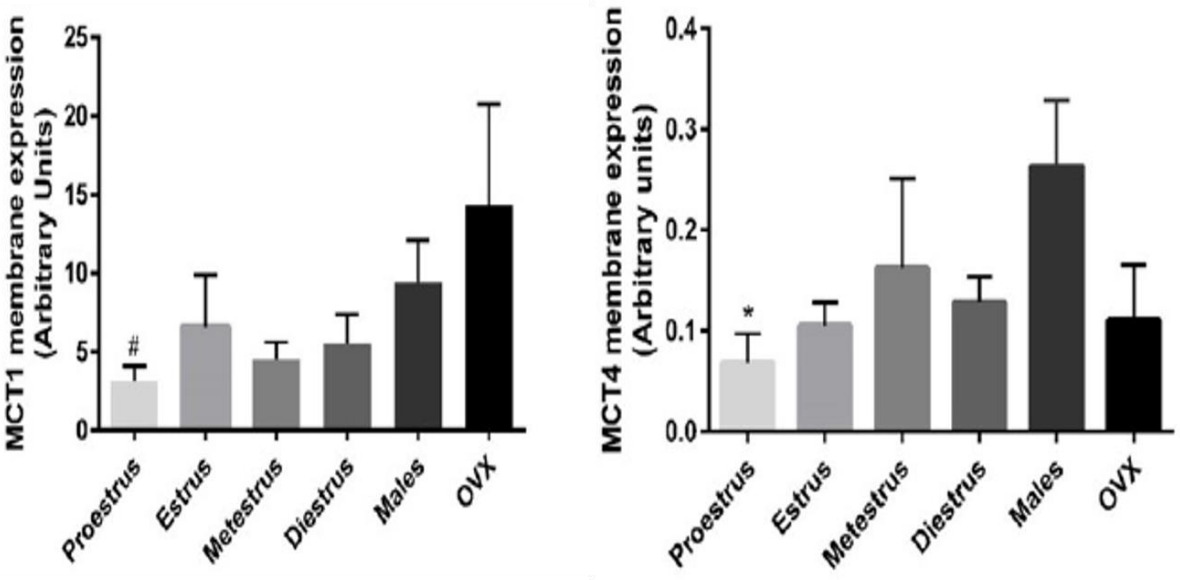

Figure 4: MCT1 and MCT4 membrane expression in the liver over the estrus cycle and in the absence of female sex hormones (from (Cao et al., 2017)). Data are presented as mean ± SD (N = 3-5). $P^{\#}$ <0.05 compared to OVX group; P^{*} <0.05 compared to male group.

1.6 Sex Differences in Expression of Other Drug Transporters

A number of drug transporters have been shown to be influenced by sex with differences in protein or mRNA expression. The oral administration of PEG 400 decreased the P-glycoprotein expression in the jejunum, ileum and colon of males, but not in the corresponding segments in females (Mai, Dou, Murdan, & Basit, 2018). In addition, estriol and ethynyl estradiol exposure resulted in concentration-dependent increases in mRNA expression of ABCB1, which encodes P-glycoprotein (Peng, Zhang, Zhang, & Wei, 2015). As well, sex differences in rat renal expression of OAT1 and OAT3 (both are p-aminohippurate transporter in kidney) have been observed after puberty, and are determined by androgens and estrogens (Ljubojevic et al., 2004). In another study, treatment of testosterone, both in male and female

rats, significantly increased both of mRNA and protein expression of OCT2 (organic cation transporter) in the kidney, while estradiol treatment moderately decreased the expression rOCT2 (Urakami, Okuda, Saito, & Inui, 2000).

Chapter 2: Thesis Objectives

GHB is widely used at nightclubs and raves, and is commonly used in drug-facilitated sexual assault. Despite the potential for illicit use and abuse in women, there is a lack of toxicokinetic data in female rats and humans. Our laboratory has previously identified sex differences in MCT expression in the liver and kidney suggesting that sex differences may be observed in GHB toxicokinetics. The LD_{50} of GHB is 1750mg/kg; a dose of 600mg/kg was selected as a mid-range dose, to avoid fatality as the variability between sexes is unknown.

The objective of this study is to evaluate sex differences and the influence of estrus cycle on GHB toxicokinetics and renal clearance after IV administration. Our hypothesis is that renal clearance and toxicokinetics will vary over the estrus cycle. We will evaluate GHB toxicokinetics following 600 mg/kg intravenous GHB over the estrus cycle in females, in the absence of female sex hormones and in male rats.

Chapter 3: Methods

3.1 Chemicals and Reagents

GHB (sodium salt) was obtained from the NIDA Drug Supply Program. Formic acid was purchased from Fisher Scientific (Fair Lawn, NJ). Deuterated GHB (GHB-d_6) was obtained from Sigma-Aldrich (St. Louis, MO). Ketamine, xylazine, and heparin were purchased from Patterson Veterinary (Saint Paul, MN). High-performance liquid chromatography (HPLC)-grade acetonitrile, methanol, and acetic acid were purchased from Fisher Scientific (Fair Lawn, NJ).

3.2 Animals

Male and female Sprague Dawley (SD) rats and ovariectomized females were obtained from Charles River at 8 weeks of age. They were housed in a temperature-controlled room with a 12-hour day/night lighting cycle and were housed individually after surgical procedures. All rats were fed standard rat chow and water *ad libitum*.

3.3 Estrus Cycle Staging

The estrus cycle typically lasts for four to five days in rats and is a repetitive, but dynamic process (Cora et al., 2015). During the estrus cycle, there are different cell types that appear and disappear throughout the process. All cell type descriptions are based on cytology slides prepared from vaginal smears which are stained by crystal violet (Manente et al., 2015).

There are three different cell types in vaginal smears (Figure 5 from (Cao et al., 2017)). Nucleated epithelial cells (arrow 1) are round to oval cells with a nucleus which can be visualized clearly (Figure 5A ,5C and 5D). In some reviews, nucleated epithelial cells are divided into large and small cells (Cora et al., 2015), but this is not necessary to assign estrus

cycle stage. Anucleated epithelial cells (arrow 2) are irregular polygonal cells without a nucleus. The pale area in the center of the cell is the position where the nucleus existed (Figure 5B, 5C and 5D). Neutrophils (arrow 3), also called leukocytes, are round nucleated cells and are the amallest cells in vaginal cytology. During the smear collection, these cells are easily broken making it difficult to visual the nuclei. The presence of neutrophils is illustrated in Figure 5C and 5D.

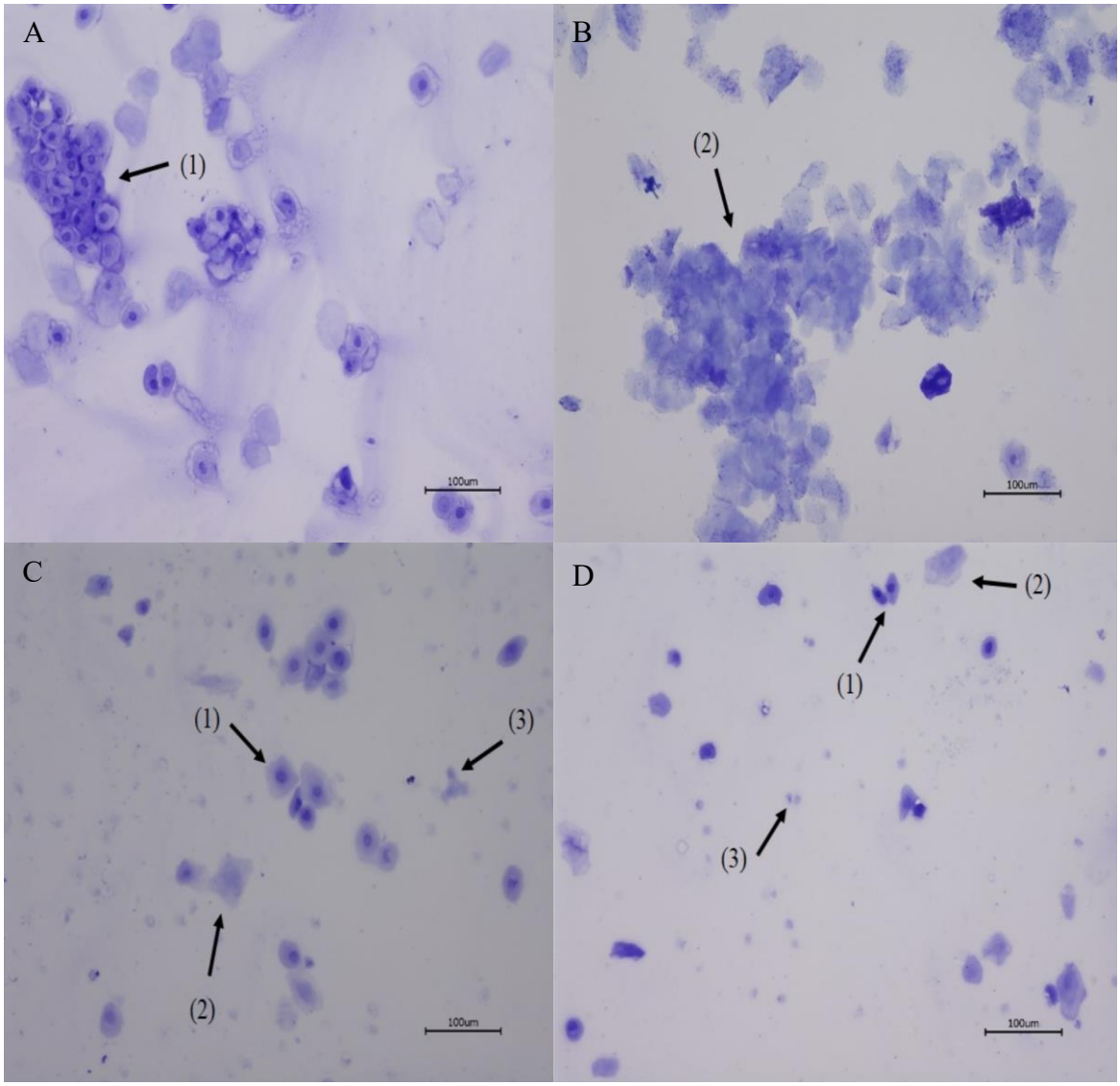

Figure 5: Different cell types in vaginal smears at 20 times magnification (from (Cao, Ng, & Felmlee, 2017)).

Estrus stage is determined according to the absence, presence, and proportion of the different cell types and cell density. Generally, the cycle can be divided into four stages: proestrus, estrus, metestrus, and diestrus. Proestrus is a short stage, averaging 14 hours in rats (Cora et al., 2015), and is characterized by the presence of predominately small, round, nucleated epithelial with moderate to low cellularity. Estrus lasts between 24 and 48 hours (Cora et al., 2015). The predominant feature of this stage is the presence of anucleated keratinized epithelial cells with high cell density. Numerous bacteria may be observed adhered to the cells or free in the background. Metestrus is a short stage of 6 - 8 hours in rats (Cora et al., 2015) and the main feature of this stage is a combination of nucleated epithelial cells, anucleated keratinized epithelial cells and neutrophils. The number of neutrophils is very high, 10 times more than the number of epithelial cells. In the late phase of metestrus, the number of different cells all decrease leading to a decrease in cell density. Diestrus is the longest stage of the estrus cycle and the duration ranges from 48 to 72 hours in rats (Cora et al., 2015). The cellularity is moderate to low with a combination of neutrophils, small and large nucleated epithelial cells, and low numbers of anucleated keratinized cells. Table 1 describes the classification of estrus cycle stages based on cell types and relative number of these cell types in vaginal smears. According to the shape, size, with or without nuclei, cell can be divided into 3 types neutrophils, nucleated epithelial cells, and anucleated keratinized epithelial cells. After imaging, based on the number of different types of cells and relative cell density, estrus cycle stage of each rat was determined daily.

Table 1**:** Basic classification of the stages of estrous cycle based on cell types and relative numbers of these cell types in vaginal smears (modified from reference (Cora, Kooistra, & Travlos, 2015)).

Stage	Neutrophils	Nucleated epithelial cells	Anucleated Keratinized epithelial cells	Relative Cell Density
Proestrus	0 to +	++ to +++	0 to +	Low to moderate
Estrus	0 to +	0 to ++	++ to +++	Moderate to high
Metestrus	+ to +++	+ to ++	+ to +++	Moderate to high
Diestrus	++ to +++	+ to ++	0 to +	Low to moderate

Note: 0 = none; + = few; ++ = moderate; +++ = high.

Collection of the vaginal cytology samples was done by vaginal lavage. To elucidate the estrus cycle length and to ensure the accuracy of each stage on the day of the pharmacokinetic study, vaginal smears were collected over at least 2 consecutive cycles between 9 am – 11 am every day. Rats were under anesthesia (isoflurane: 3 – 4 % induction and 2% maintenance) for the duration of the vaginal lavage.

3.3.1 Vaginal lavage procedure. 1) Draw up approximately 100 µl of sterile ddH_2O using a disposable pipet tip; 2) Placed the rat rear end towards you; 3) Grasp the tail and lift the rear end, and then insert the end of the ddH_2O-filled tip into vaginal canal orifice at a depth of approximately 5–10 mm in rats (Cora et al., 2015) (this step was done very gently to avoid stimulation, which may lead to pseudopregnancy in rats (Cora et al., 2015)); 4) The ddH_2O was flushed into the vagina and back out 2 to 3 times.

After lavage, the sample was placed on a microscope slide and was dried at room temperature. 0.1% crystal violet was used to stain vaginal cytology samples. A three-step staining procedure was used: 1) Placed the dry slides into 0.1% crystal violet and stain for 1 min; 2) the slide was removed and placed into sterile ddH_2O to wash it; 3) Step 2 was repeated and the slides were airdried. Cytology samples were identified using a 20 times objective of BZ-X710 microscope (Keyence, Itasca, IL). The cytology sample figures were captured by the Capture Still Images mode of BZ-X Viewer.

3.4 Surgery

A jugular vein cannula was implanted in all animals for drug administration and blood sampling. All steps were under sterilized conditions (sterilized towel and tools). Rats were administered ketamine/xylazine (90 mg/kg ketamine +10 mg/kg xylazine) to maintain the anesthetic plane during surgery. During surgical procedures, the anesthetic state was maintained by supplemental doses of anesthetic if needed. The rats were anesthetized, shaved and the skin swabbed sequentially with soap, alcohol and betadine. Two incisions were made, one on the back (between the rat's shoulder blades) for exteriorizing the jugular catheter and one on the upper right quadrant of the rat's chest for jugular vein catheterization. The subcutaneous tissue and muscle bed were gently teased apart to expose the vein. A sterile saline-filled catheter (MRE-040 tubing, OD 0.040 inch, ID 0.025 inch; Braintree Scientific) for systemic drug dosing and systemic blood sampling was implanted into the jugular vein (approximately 3 mm), anchored with silk suture (4-0), and tunneled subcutaneously to the shoulder and exteriorized between the shoulder blades. The skin incisions were sealed with surgical staples and triple antibiotic (Patterson Veterinary) was applied to the wounds. Buprenorphine (0.05 mg/kg sc) and saline (2 ml sc) were given immediately following the surgery for pain management and fluid

replacement. The rats were monitored (respiratory rate, pain reflex and the color of toe, eye and mucous membrane) every 15 minutes until they recovered and were moving freely. Cannulas were flushed with heparinized saline (40 IU/mL daily to ensure cannula patency for the toxicokinetic studies). Surgery was performed at least two days before the toxicokinetic studies.

3.5 Toxicokinetic Study Design

GHB was dissolved in doubled-distilled water (300 mg/ml) and filtered with 0.2 μm filters to ensure sterility. GHB (600 mg/kg) was administered by intravenous bolus injection via the jugular vein cannula to male, different estrus cycle stage females, and ovariectomized female Sprague-Dawley rats (n = 4 - 5 per group). Each estrus stage evaluated represents an independent group of animals. Ovariectomized females were included to evaluate toxicokinetics in the absence of sex hormones. All rats were dosed in metabolic cages with *ad libitum* access to water to allow for the simultaneous collection of blood and urine sample for up to 6 hours. The time of sedative/hypnotic effect onset (LRR) and offset (RRR) was recorded for all the animals. The LRR and RRR is the time when the animal lost or regained the ability to right itself when placed on their back. The animals were placed on their back immediately after dosing and the sedative/hypnotic effect was checked every 30 s until LRR. Blood samples (200 μl) were taken from the jugular vein cannula at different time points (10, 30, 60, 90, 120, 180, 210, 240 and 270 minutes) and transferred into heparinized 0.65 ml microcentrifuge tubes. Plasma samples were separated by centrifugation at 5000 rpm for 15 minutes at 4℃ and stored at -20℃. Urine samples were collected at 120, 240, 360 minutes, the total urine volume was determined and the sample was transferred into 15 ml centrifuge tubes and stored at -20℃.

3.6 Coordination of Studies

Animals were received, and acclimatized for at least two days before evaluation of the estrus cycle. To elucidate the estrus cycle length and to ensure the accuracy of the stage on the day of the TK/PD study, vaginal smears were collected over at least 2 consecutive cycles (about 8-10 days). Surgical implantation of the jugular cannula was done at least two days before TK studies to allow for animal recovery. Vaginal smears and estrus stage determinations were performed on the days of surgery, surgical recovery and the TK study day to make ensure the accuracy of the estrus cycle stage. Vaginal smears were always collected in the morning as described above. Animals were excluded from the study if the jugular cannula implantation was not successful (or lost patency) or if the estrus cycle stage could not be definitively assigned (ie. if there was the possibility of pseudopregnancy).

3.7 Sample Preparation

3.7.1 Plasma preparation. GHB plasma sample preparation followed a previously published method (Felmlee, Roiko, et al., 2010). GHB standard stock solutions for plasma samples were prepared in double-distilled water at the following concentrations: 10, 50, 100, 250, 1250, 2500, 5000 µg/ml. Quality control stock solutions were prepared separately at 100 and 5000 µg/ml for low QC and high QC, respectively. For standards and quality controls, 5 µl of GHB-d_6 (500 µg/ml), 5 µl of standard stock solution or QC stock solution was combined with 45 µl of blank plasma. For each unknown plasma sample, 5 µl of GHB-d_6 (500 µg/ml) was added to 50 µl plasma. Plasma samples obtained at 120 minutes or less after GHB administration were diluted 10-fold with blank plasma. 800 µl of acetonitrile with 0.1% formic acid was added to all samples and standards to precipitate plasma proteins followed by centrifugation at 10000

rpm for 20 minutes. 750 µl of the supernatant was removed, transferred to a clean microcentrifuge tube and evaporated by using CentriVap Concentrator (Labconco, Kansas City, MO) under vacuum status. Dried samples were reconstituted in 250 µl of 95:5 ddH_2O: acetonitrile with 0.1% acetic acid.

3.7.2 Urine preparation. Urine sample preparation followed a previously published method with minor modifications (Felmlee, Roiko, et al., 2010). GHB standard stock solutions for urine samples were prepared in double-distilled water at the following concentrations: 10, 20, 100, 200, 400, 1000, 2000 µg/ml. Quality control stock solutions were prepared separately at 20, 200 and 1000 µg/ml (in double-distilled water) for QC-low, QC-mid and QC-high, respectively. All urine samples and blank urine were diluted 100-fold (5 µl urine in 495 µl double-distilled water). For standards and QCs, 25 µl of diluted blank urine, 5 µl of standard or QC stock solution, 5 µl of GHB-d_6 (500 µg/ml) and 465 µl ddH_2O were combined. For unknown urine samples, 25 µl diluted sample, 5 µl GHB-d_6 (500 µg/ml) and 470 µl ddH_2O. Samples were stored at -20℃ until liquid chromatography/tandem mass spectrometry (LC/MS/MS) analysis.

3.8 LC/MS/MS Assay

GHB in plasma and urine was quantified using a validated LC/MS/MS assay described previously with minor modifications (Felmlee, Roiko, et al., 2010). The LC/MS/MS system included an Agilent 1100 series HPLC consisting of an online degasser, binary pump, and autosampler (Agilent Technologies, Santa Clara, CA) connected to MDS Sciex API 3000 triple – quadruple tandem mass spectrometer equipped with a turbo ion spray (Applied Biosystems, Foster City, CA). 20 µl of sample was injected into an Xterra MS C18 column (250 × 2.1 mm i.d., 5-µm particle size; Waters, Milford, MA). Mobile phase A was 0.1% formic acid in double-

distilled water with 5% acetonitrile. Mobile phase B was 0.1% formic in acetonitrile with 5% double-distilled water. A gradient elution with a flow rate of 200 µl/min was used to separate compounds: 100 % to 90% A over 5 min, 90% to 10% A over 2.5 min, and 10% to 100% A over 4.5 min. The total running time is 12 minutes. The mass spectrometer was operated in positive ionization mode with multiple reaction monitoring. Table 2 shows the detail of the mass spectrometer parameters of GHB and GHB-d6.

Table 2**:** Mass spectrometer parameters for MRM of GHB

Parameter (units)	GHB	GHB-d_6
Q1/Q3	105/87	111.2/93
Declustering potential (volts)	6	11
Collision energy (volts)	9	11
Collision cell exit potential (volts)	6	16

3.9 Data Analysis

Data are presented as mean ± standard deviation. Data was analyzed in GraphPad Prism 7.05 using a nonparametric one-way analysis of variance (ANOVA) with a Tukey's post hoc test to evaluate for differences between group. A P value less than 0.05 was considered statistically significant.

Non-compartmental analysis of the plasma concentration time profiles was conducted in Phoenix WinNonLin to obtain AUC_{inf} and total clearance (CL). Cumulative urinary excretion of

GHB was calculated by summing the amount excreted in urine for all three collection intervals. Fraction of drug eliminated in the urine (f_e) is the quotient of cumulative excretion divided by the product of dosage and body weight ($f_e = A_{e,inf}/(Dose*BW)$). Renal clearance ($CL_R$) was calculated as the total amount excreted in urine divided by the plasma AUC ($CL_R = A_{e,inf}/AUC$). Metabolic clearance (Cl_m) was calculated as the difference of total clearance and renal clearance [$CL_m = CL - CL_R$]. The sleep time following GHB administration was determined as the difference between RRR and LRR.

Chapter 4: Results

4.1 GHB LC-MS/MS Assay

The retention time for GHB and GHB-d6 was 3.57 minutes. The standard curve in plasma is from 1 to 500 µg/ml (Figure 6A) and in urine from 2 µg/ml to 400 µg/ml (Figure 6B), based on regression analysis (r^2 >0.99) of the peak area ratio (GHB/GHB-d_6) versus GHB concentration. Inter- and intra-day accuracy and precision based on quality control samples of the analyte were 100 ± 10%.

4.2 Estrus Staging

After imaging, the estrus stages of cycling female rats were identified by different cell types and cell density (shown in Figure 5). Figure 7 shows representative images of the four stages from the current study. Proestrus was identified by large, round nucleated epithelial cells (Figure 7A). Estrus was identified by large, anucleated keratinized epithelial cells (Figure 7B). Metestrus was identified by a high density of epithelial cells and neutrophils (Figure 7C). Diestrus was identified by a low density of epithelial cells and neutrophils (Figure 7D).

4.3 Toxicokinetic Analysis

Figure 8 shows the GHB concentration versus time profiles in plasma of individual groups after 600 mg/kg IV administration. Figure 8A is an overlay of all groups with the different color solid lines representing individual groups. It shows GHB has a non-linear toxicokinetic profiles following IV administration in all rats, regardless of sex or estrus stage, as a result of saturable metabolism and renal clearance. The C_{max} (the plasma concentration of 10 min) of males, and proestrus and estrus females are lowest compared to the other groups, while the C_{max} of diestrus females is the highest, suggesting that there may be estrus cycle dependent

differences in the initial distribution of GHB. The terminal phases have different slopes, which suggests that elimination is different between groups. As we can see, the terminal phase curve of proestrus was sharper than the other groups, whereas both the OVX and male were shallower than the cycling female suggesting greater clearance in proestrus rats. In cycling females (Figure 8B), the slope of terminal phase varies by estrus cycle stage (proestrus > estrus > metestrus > Diestrus).

Non-compartmental analysis of the plasma concentration time profiles was conducted in Phoenix WinNonLin and the results are presented in Figure 9. Total clearance (Figure 9A) was significantly influenced by sex and the estrus cycle (P 0.0466), with proestrus and estrus females trending higher than other groups. The clearance of diestrus females is the lowest of all groups with both of OVX and males having slightly higher clearance values as compared to diestrus females. The total clearance results are consistent with the calculated AUC values (Figure 9B): groups with higher clearance values had lower AUCs. While AUC values varied over the estrus cycle, after statistical analysis, there was no significant difference with one-way ANOVA (P = 0.0750). Proestrus had the lowest AUC and the highest AUC was observed in diestrus consistent with the calculated clearance values. The AUC of OVX and males were higher than all estrus stages except diestrus.

Renal clearance and the fraction of drug eliminated in the urine (f_e) are presented in Figure 10 and were calculated from urinary excretion data (Figure 9). Renal clearance varied significantly with sex and the estrus cycle (P = 0.0011); the highest renal clearance was observed in proestrus females and renal clearance declined over the subsequent stages with significantly lower renal clearance in diestrus females. Renal clearance was significantly lower in OVX and male animals as compared to proestrus females. f_e demonstrated a similar trend to renal clearance

and varied with sex and the estrus cycle (P = 0.0279), with OVX females demonstrating a significantly lower f_e as compared to proestrus females. These results are consistent with the observed sex and estrus cycle differences in AUC.

The calculated metabolic clearance is presented in Figure 11. There was no significant difference over the estrus cycle, in OVX females or males (P = 0.8066). This suggests that there are no sex or estrus cycle differences in metabolic clearance.

4.4 Pharmacodynamic Analysis

Sleep time trended lower in proestrus and estrus females consistent with the observed differences in toxicokinetics; however, the sedative/hypnotic effect of GHB showed no significance with sex or the estrus cycle (P = 0.5480) (Figure 12).

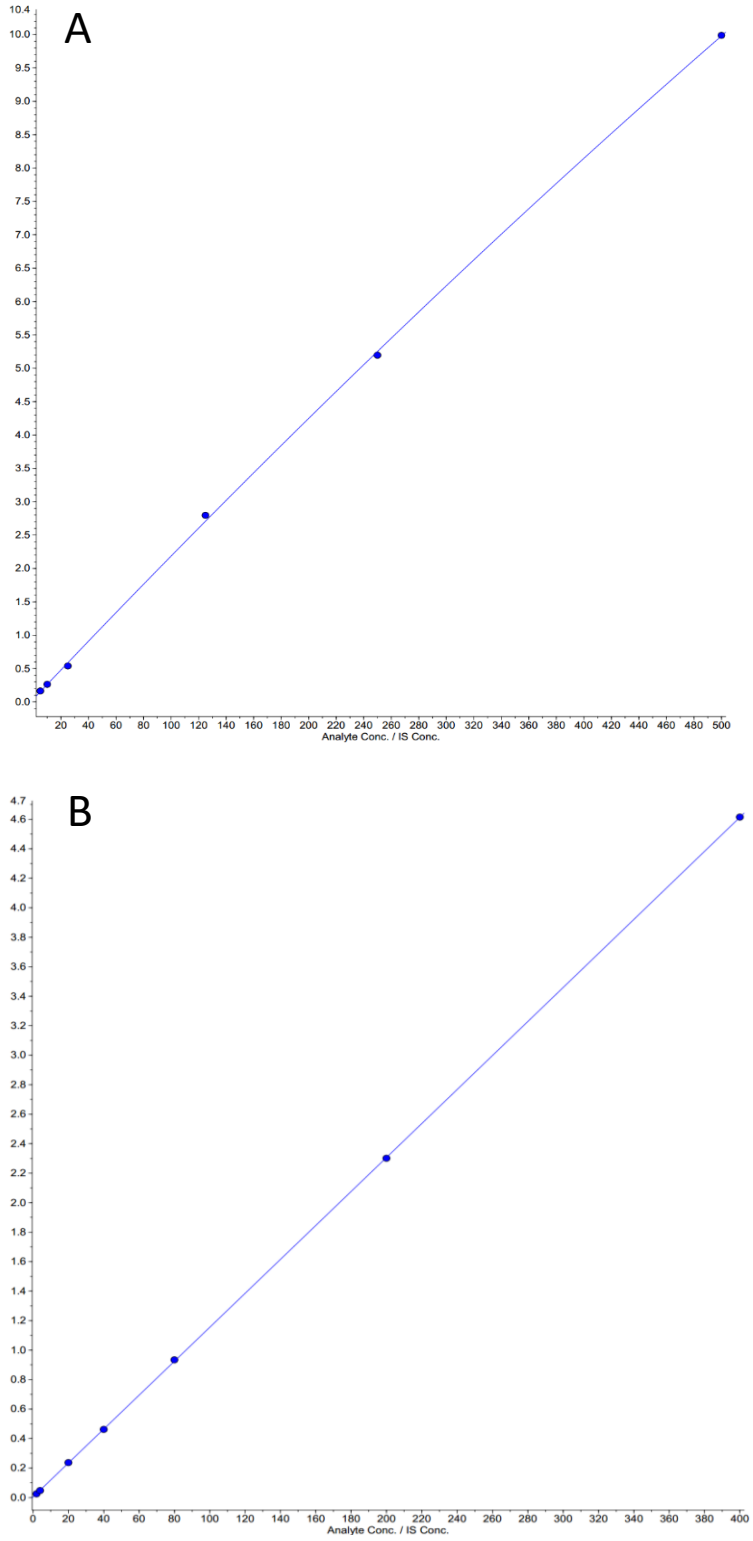

Figure 6: Standard curve of (A) GHB in plasma (r^2 = 0.9999) and (B) GHB in urine (r^2 = 1.0000).

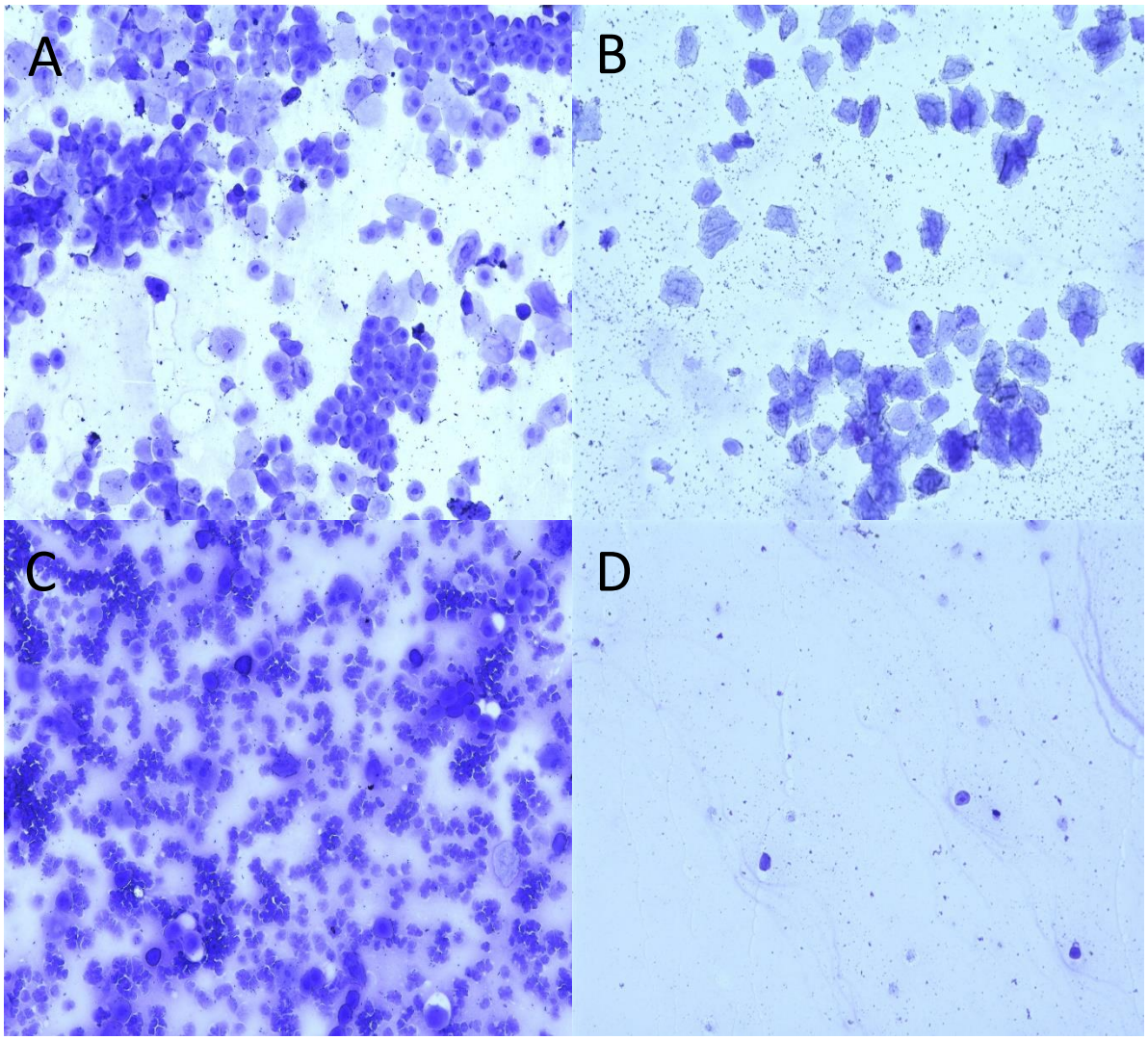

Figure 7**:** Representative vaginal smears of the four estrus stages. (A) proestrus, (B) estrus, (C) metestrus, and (D) diestrus. Stages were determined as described in the methods section and in Figure 5.

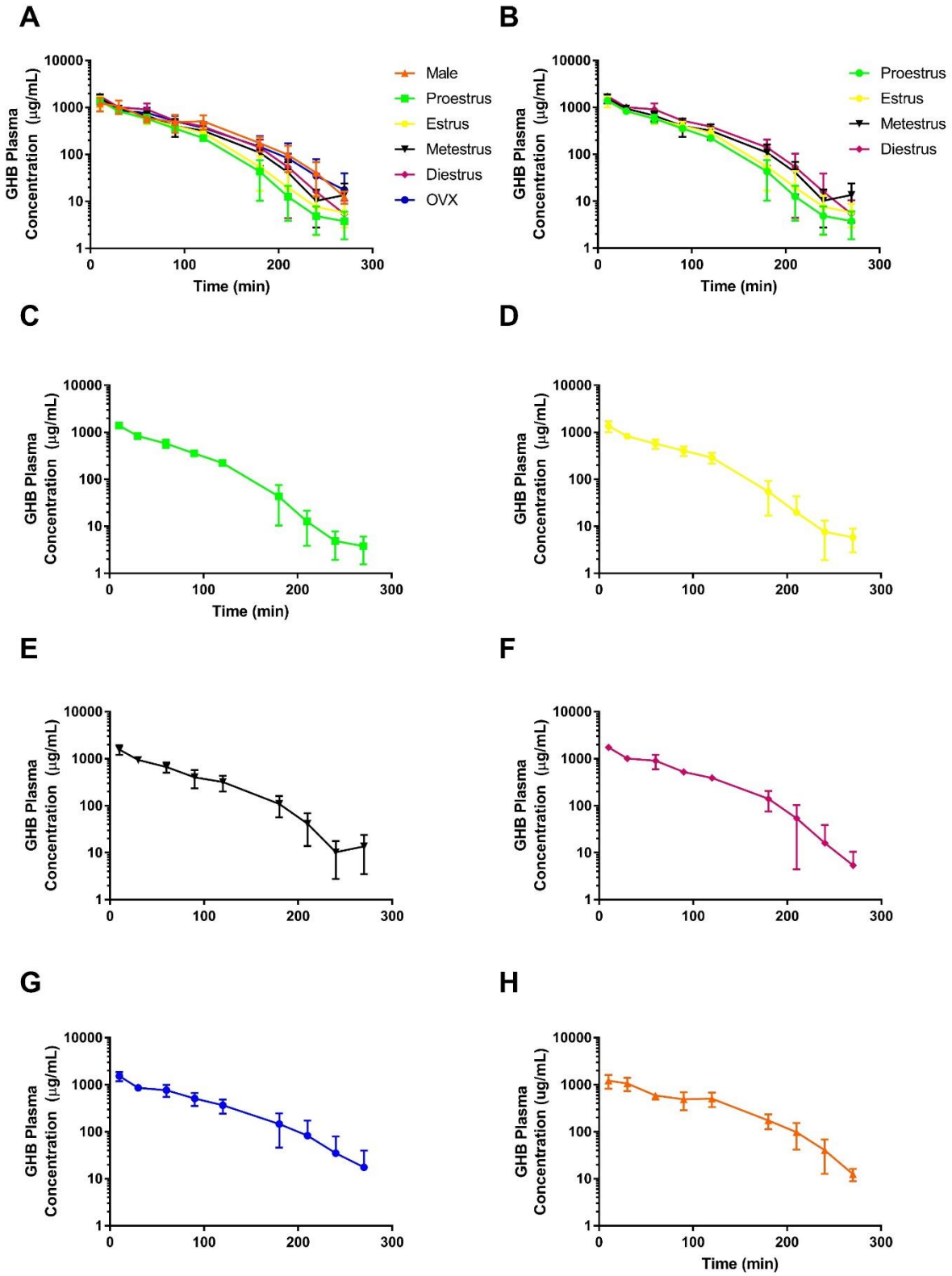

Figure 8: GHB plasma concentrations following intravenous administration of 600 mg/kg to males, OVX females and females at each estrus stage. Data presented as mean ± SD, N = 4 – 5.

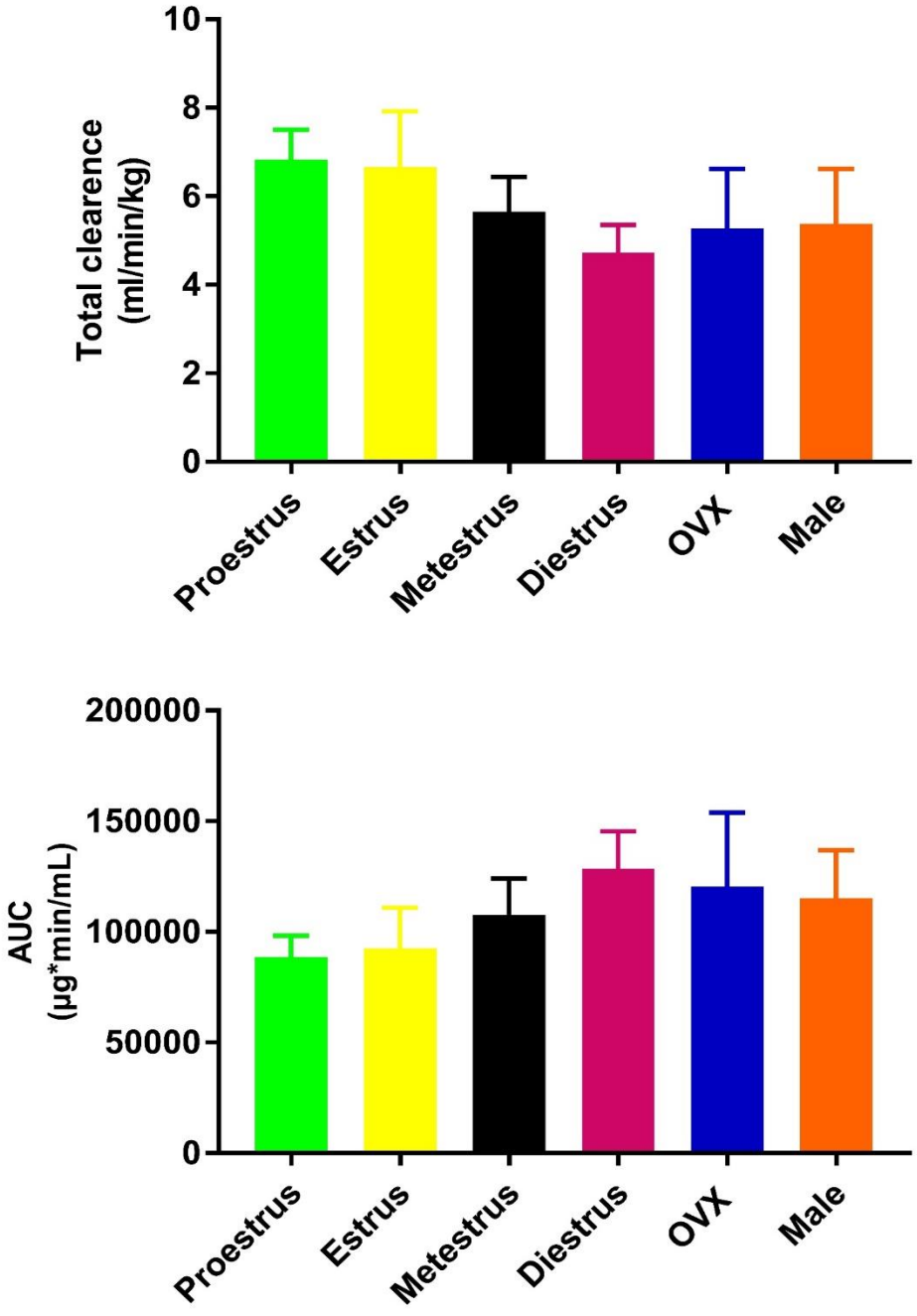

Figure 9: (A) Total clearance and (B) Area under the plasma concentration-time profile (AUC) following administration of 600 mg/kg iv in males, OVX females and females at each estrus stage. Parameters were calculated for each animal utilizing NCA analysis in Phoenix WinNonLin. Data are presented as mean ± SD, N = 4 – 5.

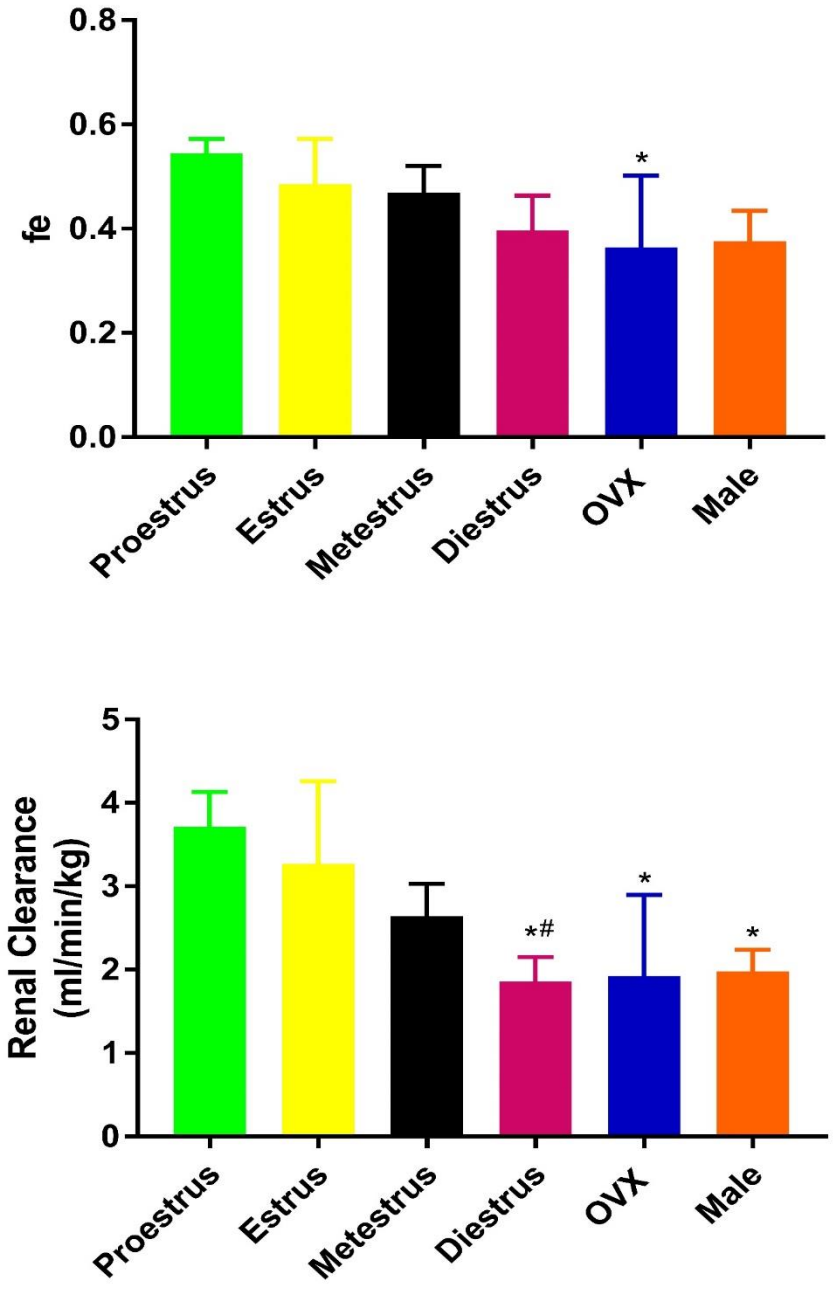

Figure 10: (A) Fraction of drug eliminated in urine (fe) and (B) renal clearance following administration of 600 mg/kg iv in males, OVX females and females at each estrus stage. Parameters were calculated for each animal based on cumulative urinary excretion of GHB utilizing the equations described in the methods section. Data are presented as mean ± SD, N = 4 – 5. *P < 0.05 compared to proestrus group. $^{\#}$P < 0.05 compared to estrus group.

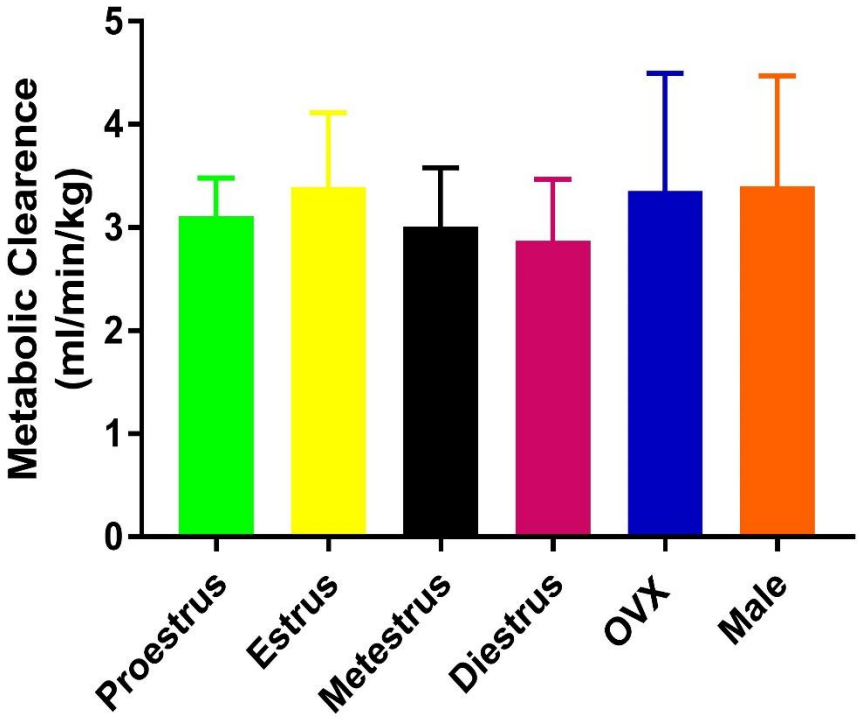

Figure 11**:** GHB metabolic clearance (CL_m) following administration of 600 mg/kg iv in males, OVX females and females at each estrus stage. CL_m was calculated as the difference between total clearance and renal clearance (as described in the methods section). Data are presented as mean ± SD, N = 4 – 5.

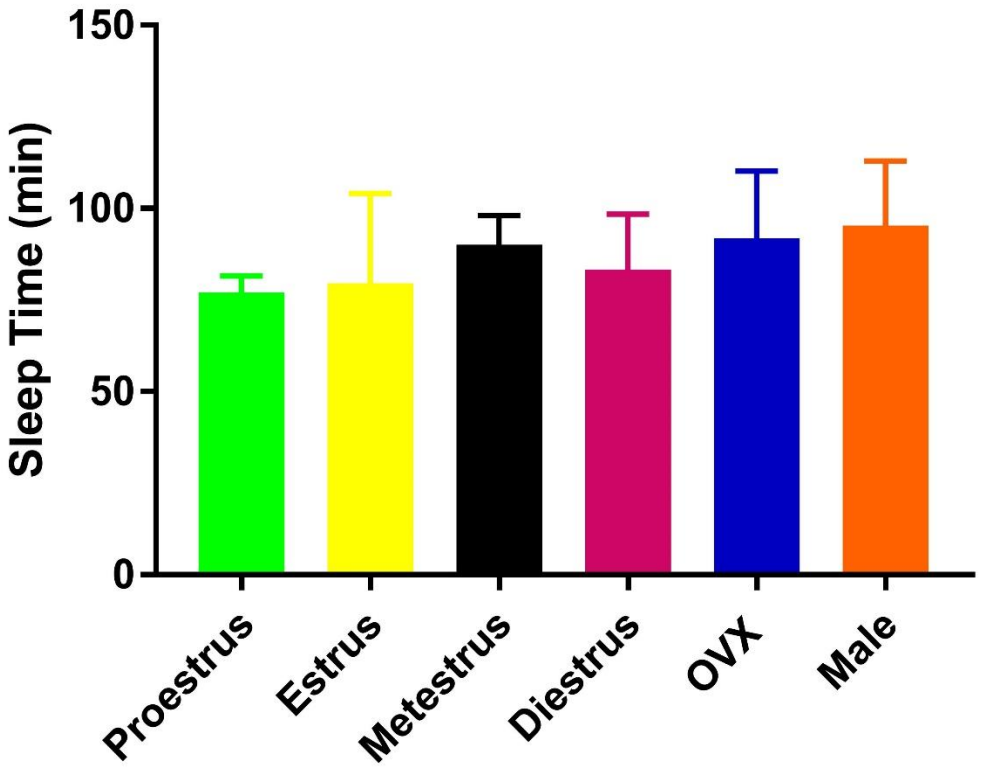

Figure 12: Sedative/hynopic effect of GHB following administration of 600 mg/kg iv in males, OVX females and females at each estrus stage. Sleep time represents the difference between RRR and LRR. Data presented as mean ± SD, N = 4 – 5.

Chapter 5: Discussion

GHB demonstrates non-linear toxicokinetics in rats following intravenous administration resulting from saturable metabolism and renal clearance (Felmlee, Wang, et al., 2010). Capacity-limited GHB renal clearance is due to saturation of active renal reabsorption via monocarboxylate transporters (Felmlee, Wang, et al., 2010; Morris et al., 2005). Membrane MCT/SMCT expression directly relates to the maximum capacity for the transporters to move GHB across the plasma membrane. Alterations in renal MCT/SMCT expression may lead to changes in GHB renal clearance and systemic drug concentrations. Previous studies have reported that MCT expression is driven by sex hormones in liver, skeletal muscle and brain (Cao et al., 2017; Enoki et al., 2006; Manente et al., 2015); however, there are no studies evaluating sex differences and the impact of sex hormones on GHB toxicokinetics. The current study is the first analysis of the influence of the estrus cycle and female sex hormones on GHB toxicokinetics. We have demonstrated that renal clearance differs between sexes, over the estrus cycle in females, and in the absence of female sex hormones. In contrast, metabolic clearance shows no difference between sexes or over the estrus cycle.

GHB demonstrates nonlinear toxicokinetics due to capacity-limited metabolism (Palatini et al., 1993) and renal reabsorption (Morris et al., 2005). Metabolic clearance is saturated and renal clearance becomes a significant route of elimination in GHB overdose. The toxicokinetic profiles in our study are consistent with previous studies reporting GHB toxicokinetics in male rats (Felmlee, Roiko, et al., 2010; Felmlee, Wang, et al., 2010; Lettieri & Fung, 1979). The concentrations which lead to death in humans (post-mortem blood levels: mean 660 mg/L) (Corkery, Loi, Claridge, Goodair, & Schifano, 2018) are lower than those that cause death in rats. However, the concentrations in current study are in the range of those seen in human

overdose. The current study shows similar total clearance in males as compared to previous literature, which indicated a GHB total clearance of 6.00 ml/min/kg and GHB renal clearance of 1.68 ml/min/kg following iv administration of 600 mg/kg (Morse et al., 2012). In addition for sedative/hypnotic effect, we demonstrated a consistent sleep time under the same overall plasma exposure (AUC) as seen in previous studies (Felmlee, Roiko, et al., 2010) with shorter sleep times observed in animals with lower plasma AUC values. As reported, the co-administration of lactate, which is the inhibitor of MCTs and SMCTs, can decrease the overall plasma exposure, increase renal clearance, and decrease sleep time, which represents the sedative/hypnotic effect (Roiko, Vijay, Felmlee, & Morris, 2013b) illustrating that modulation of MCT/SMCT-mediated renal reabsorption impacts GHB renal clearance. The dose used in the current study is relatively low fora toxicokinetic study of GHB; however, it was selected to avoid fatality (Dave, Follman, & Morris, 2017; Felmlee, Roiko, et al., 2010; Morse & Morris, 2013b; Morse et al., 2012), as it was unclear how large the differences over the estrus cycle would be. Future studies will evaluate higher doses of GHB (up to 1500 mg/kg) to evaluate the impact of sex hormones and the estrus cycle on risk of GHB-induced fatality.

MCT inhibition is a potential treatment strategy for GHB overdose by inhibiting its active renal reabsorption mediated by MCTs and SMCTs (Morris et al., 2005). To further develop this therapeutic approach, it is critical to understand the underlying sex and sex hormone-mediated differences in MCT/SMCT transport kinetics. Administration of MCT inhibitors, such as L-lactate, results in an increase in GHB renal and total clearance in rats (Felmlee et al., 2013; Morse & Morris, 2013a; Roiko et al., 2013a; Q. Wang et al., 2008). Similarly, SMCT1 is involved in renal reabsorption of lactate and pyruvate, which also function as SMCT1 inhibitors (Cui & Morris, 2009; Ganapathy et al., 2008; Gopal et al., 2007). The observed decreases in

GHB renal clearance with lactate administration are likely due to inhibition of MCTs and SMCTs. After luteolin treatment, the renal and total clearances of GHB are significantly increased because of inhibition of the MCT1-mediated renal reabsorption of GHB (Q. Wang & Morris, 2007). As well, the immunosuppressive compounds AR-C117977 and AR-C122982 are potent MCT1 inhibitors (Pahlman et al., 2013), and co-administration with GHB lead to increased GHB renal and total clearance (Vijay et al., 2015). However, GHB renal clearance remains less than filtration clearance suggesting that other monocarboxylate transporter contribute to active renal reabsorption of GHB. Due to the contribution of multiple monocarboxylate transporters to active renal reabsorption of GHB, future studies evaluating sex hormone dependent transporter expression should evaluate these multiple pathways.

MCTs are located on the basolateral membrane of renal proximal tubules (Morris & Felmlee, 2008), while SMCTs are located on the apical membrane of renal proximal tubules (Yanase, Takebe, Nio-Kobayashi, Takahashi-Iwanaga, & Iwanaga, 2008). MCTs and SMCTs function to remove GHB from the tubular fluid and return it to systemic circulation (Morris et al., 2005). Varied expression of MCTs and SMCTs in the kidney can alter renal reabsorption of GHB due to alteration in the maximum capacity for renal reabsorption (Felmlee et al., 2013). In the case of proestrus females, the total amount excreted in the urine increased likely due to decreased active renal reabsorption of GHB suggesting the proestrus females have decreased renal expression of MCTs/SMCTs. Similarly, renal clearance will be lower if MCT/SMCT expression in the kidney is greater due to an increase capacity for active renal reabsorption of GHB which leads to a decrease in overall GHB elimination (Morse & Morris, 2013a; Vijay et al., 2015). This is consistent with the observed results in males, diestrus females and OVX females. Studies are currently underway in our laboratory to quantify renal MCT/SMCT

expression in males, over the estrus cycle in females and in the absence of male and female sex hormones.

MCTs expression has been demonstrated to be regulated by sex hormones in Sertoli cells, skeletal muscle and brain (Enoki et al., 2006; Manente et al., 2015; Rato et al., 2012); however, there is minimal data in tissues involved in drug distribution. In Sertoli cells, the MCT 4 mRNA level significantly decreased in 17β-oestradiol and dihydrotestosterone treatment groups (Rato et al., 2012). Administration of testosterone increased MCT1 and MCT4 protein expression in rat skeletal muscle (Enoki et al., 2006). Oestrogen-related receptor alpha (ERRα) expression can modulate the expression of MCT1 in mice (Aveseh et al., 2015), and the induction of estrogen receptor β (ERβ) expression result in the expression of MCT4 in mesothelioma cells of mice (Aveseh et al., 2015). The absence of female sex hormones after ovariectomy (OVX) induced a decrease of MCT2 expression in brain of mice (Manente et al., 2015). Taken together these results suggest that sex hormones regulate monocarboxylate transporters; however, the observed alterations in expression differ between tissues. Previous studies in our laboratory have shown that MCT1 and MCT4 are regulated in a sex and sex hormone-dependent manner in the liver (Cao et al., 2017). MCT1 and MCT4 membrane expression is lower in proestrus females, as compared to males and OVX females (Cao et al., 2017). These expression changes are consistent with our predicted changes in renal MCT expression based on our observed renal clearance changes (renal clearance of proestrus females is the highest compared the other groups). Preliminary data from our laboratory indicates that renal MCT1 membrane expression is lower in proestrus and metestrus females as compared to males and OVX females (J. Cao and MA Felmlee, unpublished data), which is consistent with our observed renal clearance data. However, renal SMCT expression data in females over the estrus cycle is not currently available

in the literature and needs to be evaluated to predict changes in renal clearance. In addition, our preliminary data in castrated male rats demonstrated significantly higher kidney MCT1 membrane expression as compared to all females, which may lead to extensive reabsorption of GHB and a significantly lower GHB renal clearance. Such changes may lead to significantly increased systemic GHB plasma concentration corresponding to an increased risk of fatality, and accordingly castrated males should be included in future toxicokinetic studies.

There are limited studies on SMCT1 expression in response to exogenous sex hormones. Progesterone decreased protein expression of SMCT1 (Takiue, Hosoyamada, Kimura, & Saito, 2011). However, there is lack of data on renal SMCT1 and SMCT2 expression in females over the estrus cycle and in the absence of sex hormones, which should be included to predict the renal clearance in combination with MCT1 renal expression. Further, MCT and SMCT expression has not been evaluated in response to treatment with exogenous sex hormones. The contribution of individual sex hormones to the regulation of renal MCT/SMCT expression is not currently known. With respect to metabolic clearance, there is a lack of metabolic enzyme expression in response to sex hormones; however, there appears to be no sex differences in metabolic clearance.

In summary, we have demonstrated that GHB toxicokinetics and renal clearance differs between sexes, over the estrus cycle in females, and in the absence of female sex hormones following intravenous administration. GHB renal clearance varied significantly over the estrus cycles with diestrus and OVX females having significantly lower GHB renal clearance. As a moderate GHB dose was used in this study, future studies should evaluate higher GHB doses to determine differences between the sexes in GHB overdose and fatality potential. In addition,

hormone replacement studies should be conducted to confirm the role of individual sex hormones on the toxicokinetics of GHB.

References

Abanades, S., Farre, M., Segura, M., Pichini, S., Barral, D., Pacifici, R., . . . De La Torre, R. (2006). Gamma-hydroxybutyrate (GHB) in humans: pharmacodynamics and pharmacokinetics. *Ann N Y Acad Sci, 1074*, 559-576. doi:10.1196/annals.1369.065

Aveseh, M., Nikooie, R., & Aminaie, M. (2015). Exercise-induced changes in tumour LDH-B and MCT1 expression are modulated by oestrogen-related receptor alpha in breast cancer-bearing BALB/c mice. *J Physiol, 593*(12), 2635-2648. doi:10.1113/jp270463

Boscolo-Berto, R., Viel, G., Montagnese, S., Raduazzo, D. I., Ferrara, S. D., & Dauvilliers, Y. (2012). Narcolepsy and effectiveness of gamma-hydroxybutyrate (GHB): a systematic review and meta-analysis of randomized controlled trials. *Sleep Med Rev, 16*(5), 431-443. doi:10.1016/j.smrv.2011.09.001

Cao, J., Ng, M., & Felmlee, M. A. (2017). Sex Hormones Regulate Rat Hepatic Monocarboxylate Transporter Expression and Membrane Trafficking. *J Pharm Pharm Sci, 20*(1), 435-444. doi:10.18433/J3CH29

Cora, M. C., Kooistra, L., & Travlos, G. (2015). Vaginal Cytology of the Laboratory Rat and Mouse: Review and Criteria for the Staging of the Estrous Cycle Using Stained Vaginal Smears. *Toxicol Pathol, 43*(6), 776-793. doi:10.1177/0192623315570339

Corkery, J. M., Loi, B., Claridge, H., Goodair, C., & Schifano, F. (2018). Deaths in the Lesbian, Gay, Bisexual and Transgender United Kingdom Communities Associated with GHB and Precursors. *Curr Drug Metab, 19*(13), 1086-1099. doi:10.2174/1389200218666171108163817

Cui, D., & Morris, M. E. (2009). The drug of abuse gamma-hydroxybutyrate is a substrate for sodium-coupled monocarboxylate transporter (SMCT) 1 (SLC5A8): characterization of SMCT-mediated uptake and inhibition. *Drug Metab Dispos, 37*(7), 1404-1410. doi:10.1124/dmd.109.027169

Dave, R. A., Follman, K. E., & Morris, M. E. (2017). gamma-Hydroxybutyric Acid (GHB) Pharmacokinetics and Pharmacodynamics: Semi-Mechanistic and Physiologically Relevant PK/PD Model. *Aaps j, 19*(5), 1449-1460. doi:10.1208/s12248-017-0111-7

Enoki, T., Yoshida, Y., Lally, J., Hatta, H., & Bonen, A. (2006). Testosterone increases lactate transport, monocarboxylate transporter (MCT) 1 and MCT4 in rat skeletal muscle. *J Physiol, 577*(Pt 1), 433-443. doi:10.1113/jphysiol.2006.115436

Felmlee, M. A., Dave, R. A., & Morris, M. E. (2013). Mechanistic models describing active renal reabsorption and secretion: a simulation-based study. *AAPS J, 15*(1), 278-287. doi:10.1208/s12248-012-9437-3

Felmlee, M. A., Morse, B. L., Follman, K. E., & Morris, M. E. (2017). The Drug of Abuse Gamma-Hydroxybutyric Acid Exhibits Tissue-Specific Nonlinear Distribution. *AAPS J, 20*(1), 21. doi:10.1208/s12248-017-0180-7

Felmlee, M. A., Roiko, S. A., Morse, B. L., & Morris, M. E. (2010). Concentration-effect relationships for the drug of abuse gamma-hydroxybutyric acid. *J Pharmacol Exp Ther, 333*(3), 764-771. doi:jpet.109.165381 [pii]

10.1124/jpet.109.165381

Felmlee, M. A., Wang, Q., Cui, D., Roiko, S. A., & Morris, M. E. (2010). Mechanistic toxicokinetic model for gamma-hydroxybutyric acid: inhibition of active renal reabsorption as a potential therapeutic strategy. *AAPS J, 12*(3), 407-416. doi:10.1208/s12248-010-9197-x

Ferrara, S. D., Zotti, S., Tedeschi, L., Frison, G., Castagna, F., Gallimberti, L., . . . Palatini, P. (1992). Pharmacokinetics of gamma-hydroxybutyric acid in alcohol dependent patients after single and repeated oral doses. *Br J Clin Pharmacol, 34*(3), 231-235.

Fung, H. L., Tsou, P. S., Bulitta, J. B., Tran, D. C., Page, N. A., Soda, D., & Mi Fung, S. (2008). Pharmacokinetics of 1,4-butanediol in rats: bioactivation to gamma-hydroxybutyric acid, interaction with ethanol, and oral bioavailability. *AAPS J, 10*(1), 56-69. doi:10.1208/s12248-007-9006-3

Ganapathy, V., Thangaraju, M., Gopal, E., Martin, P. M., Itagaki, S., Miyauchi, S., & Prasad, P. D. (2008). Sodium-coupled monocarboxylate transporters in normal tissues and in cancer. *AAPS J, 10*(1), 193-199. doi:10.1208/s12248-008-9022-y

Gopal, E., Umapathy, N. S., Martin, P. M., Ananth, S., Gnana-Prakasam, J. P., Becker, H., . . . Prasad, P. D. (2007). Cloning and functional characterization of human SMCT2 (SLC5A12) and expression pattern of the transporter in kidney. *Biochim Biophys Acta, 1768*(11), 2690-2697. doi:10.1016/j.bbamem.2007.06.031

Haim, S., Shakhar, G., Rossene, E., Taylor, A. N., & Ben-Eliyahu, S. (2003). Serum levels of sex hormones and corticosterone throughout 4- and 5-day estrous cycles in Fischer 344 rats and their simulation in ovariectomized females. *J Endocrinol Invest, 26*(10), 1013-1022. doi:10.1007/BF03348201

Halestrap, A. P. (2013). The SLC16 gene family - structure, role and regulation in health and disease. *Mol Aspects Med, 34*(2-3), 337-349. doi:10.1016/j.mam.2012.05.003

Halestrap, A. P., & Price, N. T. (1999). The proton-linked monocarboxylate transporter (MCT) family: structure, function and regulation. *Biochem J, 343 Pt 2*, 281-299.

Iwanaga, T., & Kishimoto, A. (2015). Cellular distributions of monocarboxylate transporters: a review. *Biomed Res, 36*(5), 279-301. doi:10.2220/biomedres.36.279

Jackson, V. N., Price, N. T., & Halestrap, A. P. (1995). cDNA cloning of MCT1, a monocarboxylate transporter from rat skeletal muscle. *Biochim Biophys Acta, 1238*(2), 193-196.

Jones, R. S., & Morris, M. E. (2016). Monocarboxylate Transporters: Therapeutic Targets and Prognostic Factors in Disease. *Clin Pharmacol Ther, 100*(5), 454-463. doi:10.1002/cpt.418

Kantrowitz, J. T., Citrome, L., & Javitt, D. C. (2009). A review of tolerability and abuse liability of gamma-hydroxybutyric acid for insomnia in patients with schizophrenia. *Clin Ther, 31 Pt 1*, 1360-1373. doi:10.1016/j.clinthera.2009.07.005

Lebron-Milad, K., & Milad, M. R. (2012). Sex differences, gonadal hormones and the fear extinction network: implications for anxiety disorders. *Biol Mood Anxiety Disord, 2*, 3. doi:10.1186/2045-5380-2-3

Lettieri, J. T., & Fung, H. L. (1979). Dose-dependent pharmacokinetics and hypnotic effects of sodium gamma-hydroxybutyrate in the rat. *J Pharmacol Exp Ther, 208*(1), 7-11.

Li, H., Myeroff, L., Smiraglia, D., Romero, M. F., Pretlow, T. P., Kasturi, L., . . . Markowitz, S. D. (2003). SLC5A8, a sodium transporter, is a tumor suppressor gene silenced by methylation in human colon aberrant crypt foci and cancers. *Proc Natl Acad Sci U S A, 100*(14), 8412-8417. doi:10.1073/pnas.1430846100

Ljubojevic, M., Herak-Kramberger, C. M., Hagos, Y., Bahn, A., Endou, H., Burckhardt, G., & Sabolic, I. (2004). Rat renal cortical OAT1 and OAT3 exhibit gender differences determined by both androgen stimulation and estrogen inhibition. *Am J Physiol Renal Physiol, 287*(1), F124-138. doi:10.1152/ajprenal.00029.2004

Mai, Y., Dou, L., Murdan, S., & Basit, A. W. (2018). An animal's sex influences the effects of the excipient PEG 400 on the intestinal P-gp protein and mRNA levels, which has implications for oral drug absorption. *Eur J Pharm Sci, 120*, 53-60. doi:10.1016/j.ejps.2018.04.021

Manente, A. G., Pinton, G., Zonca, S., Cilli, M., Rinaldi, M., Daga, A., . . . Moro, L. (2015). Intracellular lactate-mediated induction of estrogen receptor beta (ERbeta) in biphasic malignant pleural mesothelioma cells. *Oncotarget, 6*(28), 25121-25134. doi:10.18632/oncotarget.4486

Morris, M. E., & Felmlee, M. A. (2008). Overview of the proton-coupled MCT (SLC16A) family of transporters: characterization, function and role in the transport of the drug of abuse gamma-hydroxybutyric acid. *AAPS J, 10*(2), 311-321. doi:10.1208/s12248-008-9035-6

Morris, M. E., Hu, K., & Wang, Q. (2005). Renal clearance of gamma-hydroxybutyric acid in rats: increasing renal elimination as a detoxification strategy. *J Pharmacol Exp Ther, 313*(3), 1194-1202. doi:10.1124/jpet.105.083253

Morris, M. E., Morse, B. L., Baciewicz, G. J., Tessena, M. M., Acquisto, N. M., Hutchinson, D. J., & Dicenzo, R. (2011). Monocarboxylate Transporter Inhibition with Osmotic Diuresis Increases gamma-Hydroxybutyrate Renal Elimination in Humans: A Proof-of-Concept Study. *J Clin Toxicol, 1*(2), 1000105. doi:10.4172/2161-0495.1000105

Morse, B. L., & Morris, M. E. (2013a). Effects of monocarboxylate transporter inhibition on the oral toxicokinetics/toxicodynamics of gamma-hydroxybutyrate and gamma-butyrolactone. *J Pharmacol Exp Ther, 345*(1), 102-110. doi:10.1124/jpet.112.202796

Morse, B. L., & Morris, M. E. (2013b). Toxicokinetics/Toxicodynamics of gamma-hydroxybutyrate-ethanol intoxication: evaluation of potential treatment strategies. *J Pharmacol Exp Ther, 346*(3), 504-513. doi:10.1124/jpet.113.206250

Morse, B. L., Vijay, N., & Morris, M. E. (2012). gamma-Hydroxybutyrate (GHB)-induced respiratory depression: combined receptor-transporter inhibition therapy for treatment in GHB overdose. *Mol Pharmacol, 82*(2), 226-235. doi:10.1124/mol.112.078154

Pahlman, C., Qi, Z., Murray, C. M., Ferguson, D., Bundick, R. V., Donald, D. K., & Ekberg, H. (2013). Immunosuppressive properties of a series of novel inhibitors of the monocarboxylate transporter MCT-1. *Transpl Int, 26*(1), 22-29. doi:10.1111/j.1432-2277.2012.01579.x

Palatini, P., Tedeschi, L., Frison, G., Padrini, R., Zordan, R., Orlando, R., . . . Ferrara, S. D. (1993). Dose-dependent absorption and elimination of gamma-hydroxybutyric acid in healthy volunteers. *Eur J Clin Pharmacol, 45*(4), 353-356.

Peng, R., Zhang, H., Zhang, Y., & Wei, D. Y. (2015). Effects of the ABCB1 (1199G > A) Polymorphism on Steroid Sex Hormone-Induced P-Glycoprotein Expression, ATPase Activity, and Hormone Efflux. *Med Sci (Basel), 3*(4), 124-137. doi:10.3390/medsci3040124

Rato, L., Alves, M. G., Socorro, S., Carvalho, R. A., Cavaco, J. E., & Oliveira, P. F. (2012). Metabolic modulation induced by oestradiol and DHT in immature rat Sertoli cells cultured in vitro. *Biosci Rep, 32*(1), 61-69. doi:10.1042/bsr20110030

Roiko, S. A., Felmlee, M. A., & Morris, M. E. (2012). Brain uptake of the drug of abuse gamma-hydroxybutyric acid in rats. *Drug Metab Dispos, 40*(1), 212-218. doi:10.1124/dmd.111.041749

Roiko, S. A., Vijay, N., Felmlee, M. A., & Morris, M. E. (2013a). Brain extracellular gamma-hydroxybutyrate concentrations are decreased by L-lactate in rats: role in the treatment of overdoses. *Pharm Res, 30*(5), 1338-1348. doi:10.1007/s11095-013-0973-z

Roiko, S. A., Vijay, N., Felmlee, M. A., & Morris, M. E. (2013b). Brain extracellular γ-hydroxybutyrate concentrations are decreased by L-lactate in rats: role in the treatment of overdoses. *Pharm Res, 30*(5), 1338-1348. doi:10.1007/s11095-013-0973-z

Schep, L. J., Knudsen, K., Slaughter, R. J., Vale, J. A., & Megarbane, B. (2012). The clinical toxicology of gamma-hydroxybutyrate, gamma-butyrolactone and 1,4-butanediol. *Clin Toxicol (Phila), 50*(6), 458-470. doi:10.3109/15563650.2012.702218

Schwartz, C. E., & Stevenson, R. E. (2007). The MCT8 thyroid hormone transporter and Allan-Herndon-Dudley syndrome. *Best Pract Res Clin Endocrinol Metab, 21*(2), 307-321. doi:10.1016/j.beem.2007.03.009

Shannon, M., & Quang, L. S. (2000). Gamma-hydroxybutyrate, gamma-butyrolactone, and 1,4-butanediol: a case report and review of the literature. *Pediatr Emerg Care, 16*(6), 435-440.

Srinivas, S. R., Gopal, E., Zhuang, L., Itagaki, S., Martin, P. M., Fei, Y. J., . . . Prasad, P. D. (2005). Cloning and functional identification of slc5a12 as a sodium-coupled low-affinity transporter for monocarboxylates (SMCT2). *Biochem J, 392*(Pt 3), 655-664. doi:10.1042/bj20050927

Takiue, Y., Hosoyamada, M., Kimura, M., & Saito, H. (2011). The effect of female hormones upon urate transport systems in the mouse kidney. *Nucleosides Nucleotides Nucleic Acids, 30*(2), 113-119. doi:10.1080/15257770.2010.551645

Urakami, Y., Okuda, M., Saito, H., & Inui, K. (2000). Hormonal regulation of organic cation transporter OCT2 expression in rat kidney. *FEBS Lett, 473*(2), 173-176.

Vijay, N., Morse, B. L., & Morris, M. E. (2015). A Novel Monocarboxylate Transporter Inhibitor as a Potential Treatment Strategy for gamma-Hydroxybutyric Acid Overdose. *Pharm Res, 32*(6), 1894-1906. doi:10.1007/s11095-014-1583-0

Wang, Q., & Morris, M. E. (2007). Flavonoids modulate monocarboxylate transporter-1-mediated transport of gamma-hydroxybutyrate in vitro and in vivo. *Drug Metab Dispos, 35*(2), 201-208. doi:10.1124/dmd.106.012369

Wang, Q., Wang, X., & Morris, M. E. (2008). Effects of L-lactate and D-mannitol on gamma-hydroxybutyrate toxicokinetics and toxicodynamics in rats. *Drug Metab Dispos, 36*(11), 2244-2251. doi:10.1124/dmd.108.022996

Wang, X., Wang, Q., & Morris, M. E. (2008). Pharmacokinetic interaction between the flavonoid luteolin and gamma-hydroxybutyrate in rats: potential involvement of monocarboxylate transporters. *AAPS J, 10*(1), 47-55. doi:10.1208/s12248-007-9001-8

Wang, Y. G., Swick, T. J., Carter, L. P., Thorpy, M. J., & Benowitz, N. L. (2009). Safety overview of postmarketing and clinical experience of sodium oxybate (Xyrem): abuse, misuse, dependence, and diversion. *J Clin Sleep Med, 5*(4), 365-371.

White, C. M. (2017). Pharmacologic, Pharmacokinetic, and Clinical Assessment of Illicitly Used gamma-Hydroxybutyrate. *J Clin Pharmacol, 57*(1), 33-39. doi:10.1002/jcph.767

Yanase, H., Takebe, K., Nio-Kobayashi, J., Takahashi-Iwanaga, H., & Iwanaga, T. (2008). Cellular expression of a sodium-dependent monocarboxylate transporter (Slc5a8) and the MCT family in the mouse kidney. *Histochem Cell Biol, 130*(5), 957-966. doi:10.1007/s00418-008-0490-z